applied sciences

MDPI

Article

Using Geochemical and Environmental Isotopic Tracers to Evaluate Groundwater Recharge and Mineralization Processes in Qena Basin, Eastern Nile Valley, Egypt

Amira Reda [1], Mustafa Eissa [1,2,*], Ibrahim El Shamy [3], Elissavet Dotsika [4], Mostafa Saied [1] and Sayed Mosaad [3]

[1] Desert Research Center, Division of Water Resources and Arid Land, Hydrogeochemistry Department, Cairo P.O. Box 11753, Egypt
[2] Center for Water Supply Studies, Texas A&M University-Corpus Christi, Corpus Christi, TX 78412, USA
[3] Faculty of Sciences, Geology Department, Helwan University, Helwan P.O. Box 11795, Egypt
[4] Stable Isotope Unit, National Centre for Scientific Research (N.C.S.R.) "Demokritos", Institute of Nanoscience and Nanotechnology, Patriarchou Gregoriou (End) and Neapoleos Street, 15341 Agia Paraskevi, Greece
* Correspondence: mustafa.eissa@drc.gov.eg

Abstract: The Qena basin (16,000 km^2) represents one of the largest dry valleys located in the arid Eastern Desert of Egypt. Groundwater resources in this watershed are scarce due to limited recharge from annual precipitation. Hydrogeochemistry and environmentally stable isotopes were utilized to determine the main sources of recharge and geochemical processes affecting groundwater quality. The studied basin comprises three main groundwater aquifers: the Quaternary aquifer, the Post-Nubian aquifer (PNA) of the Paleocene-Eocene age, and the Nubian Sandstone aquifer (NSA) of the Lower Cretaceous age. Groundwater types vary from fresh to brackish groundwater. The groundwater salinity of the Quaternary aquifer ranges from 426 to 9975 mg/L with an average of 3191 mg/L, the PNA's groundwater salinity ranges from 1134 to 6969 mg/L with an average of 3760 mg/L, and the NSA's groundwater salinity ranges from 1663 to 1737 mg/L with an average of 1692 mg/L. The NSA's groundwater is relatively depleted of stable isotopes' signatures (ranges: δ^{18}O from −9‰ to −4.81‰; δ^2H from −71‰ to −33.22‰), whereas the Quaternary aquifer's groundwater is relatively enriched (ranges: δ^{18}O from −5.51 to +4.70‰; δ^2H from −40.87 to +37.10‰). Geochemical and isotopic investigations reveal that the NSA groundwater is a paleo-water recharged in a cooler climate. In contrast, the upstream Quaternary groundwater receives considerable recharge from recent meteoric water and upward leakage from the artesian NSA. The downstream Quaternary aquifer in the delta of the Qena basin is composed of original groundwater mixed with recharge from the River Nile. Isotopic analysis confirms that the PNA's groundwater recharge (ranges: δ^{18}O from −5.90 to −0.10; δ^2H −58.21 to −7.10‰) mainly originates from upward leakage from the NSA under the artesian condition and seepage from the upper unconfined Quaternary aquifer. NETPATH geochemical model results show that water–rock interaction, evaporation, and mixing are the main geochemical and physical processes controlling the groundwater quality. NSA groundwater has a significant regional extension and salinity suitable for use in expanding agricultural projects; it should be well managed for sustainable development.

Keywords: hydrogeochemistry; environmental isotopes; Qena basin; geochemical models

check for updates

Citation: Reda, A.; Eissa, M.; Shamy, I.E.; Dotsika, E.; Saied, M.; Mosaad, S. Using Geochemical and Environmental Isotopic Tracers to Evaluate Groundwater Recharge and Mineralization Processes in Qena Basin, Eastern Nile Valley, Egypt. *Appl. Sci.* **2022**, *12*, 8391. https://doi.org/10.3390/app12178391

Academic Editor: Valerio Comerci

Received: 1 January 2022
Accepted: 11 August 2022
Published: 23 August 2022

1. Introduction

In arid regions, groundwater represents one of the primary sources of water for agricultural and other development projects, especially in remote watersheds. Wadi Qena is located in the Eastern Desert of Egypt, draining toward the Nile valley. It is considered a promising area for agricultural and sustainable development projects. Wadi Qena is bound by the Nile River to the west and the Red Sea mountains series ridges to the East. The Wadi flows from north to south, unlike other major Egyptian Nile drainage systems, which are generally oriented from east to west [1]; the Wadi covers an area of 16,000 km^2 with an average width of 75 km [2]. Wadi Qena lies between latitudes 26°15′00″ N and 28°15′00″ N and between longitudes 32°15′00″ E and 33°30′33″ E (Figure 1). It is easily accessible through a road network, connecting the densely populated Nile Valley with the touristic Red Sea Province. Wadi Qena receives 1.4×10^8 m^3 annual precipitation, which feeds the aquifers [3]. In addition, it has mostly flatlands that are suitable for land development in downstream regions. Climatic data reveals that the maximum relative humidity varies from 53% in winter to 29% in summer. The average maximum temperature is approximately 23 °C in winter and 44 °C in summer, whereas the minimum is approximately 10 °C in winter and 22 °C in summer [4]. The average maximum recorded evaporation rate is 17.63 mm during June, whereas the average minimum recorded evaporation rate is 4.54 mm in December (Egyptian Meteorological Department 1935–2000).

In the past decade, Wadi Qena has experienced rapid development, primarily related to agricultural projects that resulted in increased demand for groundwater resources. These groundwaters are exploited from three main aquifers: the Nubian Sandstone aquifer (NSA), the Post-Nubian carbonate aquifer (PNA), and the alluvial Quaternary aquifer [5,6].

Understanding the main processes controlling groundwater chemistry and recharge is important for sustainable management of groundwater resources used in this arid watershed. In this respect, gathering information related to recharge mechanisms, geochemical characteristics, and groundwater evolution is necessary for sustainable groundwater use [7–9]. Variations in groundwater geochemistry within the aquifers result from salt leaching in the aquifer matrix, cation exchange processes, and the length of time the groundwater remains in the aquifer [10]. However, local geology, the degree of rock weathering, the quality of recharge water, and inputs from sources other than rock–water interaction can influence groundwater chemistry throughout its flow path [11–13]. Moreover, accurately identifying the groundwater recharge mechanism and its sources using conventional hydrogeological methods is difficult [7,8,14]. In arid regions, integrating these methods with geochemical and environmental isotopic tracers can be utilized to understand the geochemistry of the groundwater, recharge sources, and to determine evolutionary processes [9,15]. It can also provide relevant information regarding the origin of groundwater mineralization [16]. Geochemical indicators and environmental isotopes offer unique and valuable insights regarding the origin of groundwater and its movements. They can also be used to effectively characterize tracing of contaminants and solute transport in groundwater [17]. They allow quantitative evaluation of mixing and other physical processes such as evaporation and isotopic exchange in hydrogeologic systems [18]. These integrations have been applied in many arid areas, including Australia, China, Tunisia, Saudi Arabia, and Egypt [15–17,19–22].

The main goal of this study is to utilize hydrogeochemical data and isotopic tracers, in addition to geochemical modeling, to (1) assess the geochemical processes controlling groundwater evolution, (2) investigate recharge sources and hydrogeochemical relations between the three principal groundwater aquifers, and (3) identify the mineralization sources that deteriorate groundwater quality.

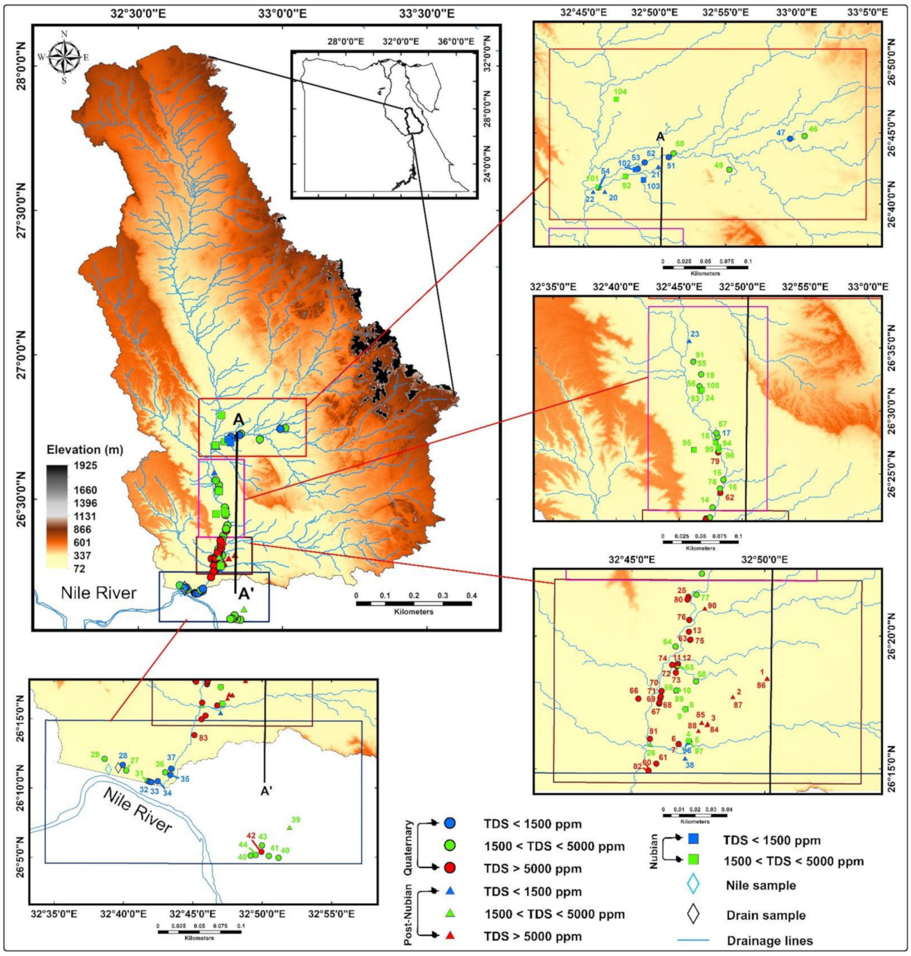

Figure 1. Location of groundwater samples. Samples 1 to 48 were collected in November 2018; samples 49 to 104 were collected later [21,22].

2. Geomorphology, Geology, and Hydrogeology

The study area comprises three main geomorphologic units (Figure 2): mountains, plateaus, and depressions [5,23,24]. The Red Sea mountainous terrains are located in the east and are composed mainly of igneous and metamorphic rocks. The plateaus consist of El Maaza limestone and El Ababda sandstone highlands. The limestone plateau occupies the western portion of the studied basin, and the sandstone plateau breaks up into low ridges and isolated hills [25]. The characteristics of these elevated areas have notable impacts on the hydrogeologic setting [23,24]. The morphotectonic depression represents one of the most noticeable topographical features in the basin, a wide lowland that extends from the northern portion of Wadi Qena to the north of the Qena-Safaga road, linking the Qena district with the Red Sea coast.

The Qena basin stratigraphy is composed of Precambrian (igneous and metamorphic) rocks overlain by Cretaceous to Quaternary sedimentary successions (Figure 2). The stratigraphic sequence consists of rock units [1,26–31] arranged from base to top as indicated in Figure 2: (1) Cretaceous, represented by Wadi Qena, Galala, Umm Omeiyied, Abu Aggag, Hawashiya, Quseir variegated shale, Duwi, Rakhiyat, and Sudr formations; (2) Paleocene, represented by Dakhla, Tarawan, and Esna formations; (3) Early Eocene, represented by the Thebes formation, and (4) undifferentiated Pliocene deposits beside the alluvial Quaternary sediments. The Wadi Qena basin was affected by shear faults, folds, and fractures, which are attributed to the Pan African orogeny and a series of tectonic reactivations, mostly during the Cretaceous and Oligocene eras [32–35].

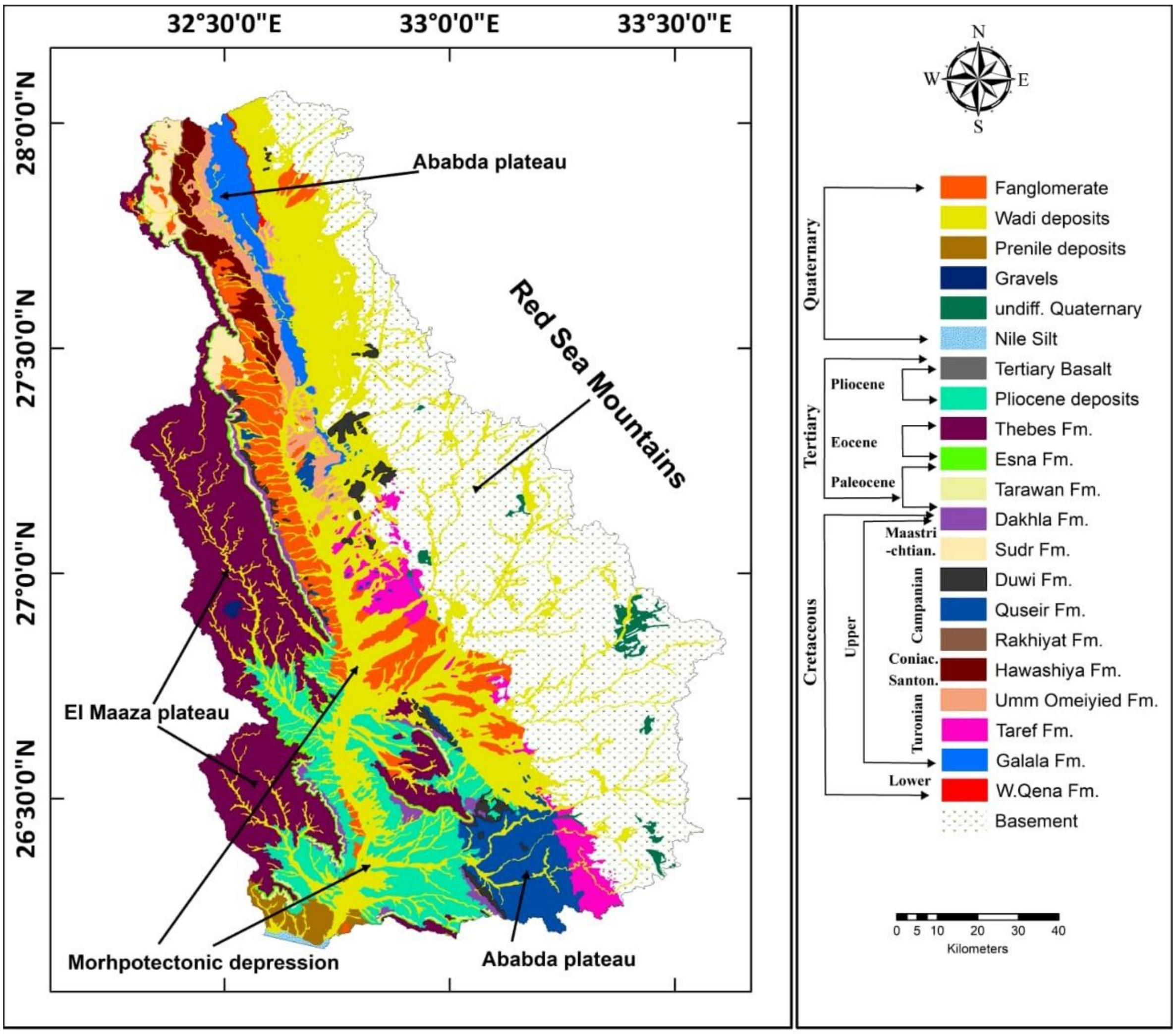

Figure 2. Wadi Qena geological map [36].

The groundwater is exploited from the Quaternary aquifer, the PNA, and the NSA (Aggour 1997 [5]). The Quaternary aquifer at Wadi Qena is the main groundwater source for irrigation; it is composed of gravel, coarse to fine sand, and conglomerates; its thickness increases downstream, attaining approximately 100 m (Figure 3; [5,37,38]. The aquifer is characterized by unconfined conditions; the water depth ranges from 1.9 to 20 m (Table 1), the maximum penetration depth from the ground surface elevation is 28 m, and the groundwater generally flows from northeast to southwest [25]. The Post-Nubian aquifer (PNA) contains water bearing limestones and sandstones of the Pliocene and/or Eocene ages. The groundwater is characterized by free water table conditions, the depth to groundwater level (DTW) ranges from 28 to 76 m, and the maximum groundwater well total depth (TD) is 200 m (Table 1). Figure 3 shows that the PNA aquifer is directly overlain by the Quaternary aquifer, where it is not separated by a confining layer of shale or clay sheets. Hence, mixing may occur naturally or be induced by pumping, affecting the groundwater chemistry. The NSA is formed mainly of sandstone intercalated with shale interbeds of the lower cretaceous age, and is considered one of the primary groundwater sources. The groundwater in the NSA is confined by impervious Quseir variegated shale overlying the aquifer [5]. The groundwater flows from northeast to southwest [25].

Table 1. Hydrogeological parameters and geochemical analyses of groundwater samples collected from the Qena basin during the November 2018 field trip.

No.	Aquifer	pH	DTW (m)	TD (m)	Temp (°C)	DO	TDS	Ca	Mg	Na	K	CO_3	HCO_3	SO_4	Cl	Si	NO_3
							mg/L										
5	Quaternary	6.8	2.5	4	24.1	2.85	2716	123	35	760	36	0	177	850	824	12.5	9.80
7	Quaternary	7.2	3	4	25	2.13	8564	478	290	2150	47	0	195	1926	3574	9.8	12.60
9	Quaternary	7.8	3	6	22.6	3.24	3059	96	58	960	24	18	226	475	1316	11.2	11.20
11	Quaternary	7.4	4	5	24.5	3.4	7593	517	290	1750	23	0	98	1985	2979	15.6	14.00
12	Quaternary	7.6	–	–	25.7	3.14	6226	517	242	1350	23	6	67	1423	2631	8.2	12.60
13	Quaternary	7.1	5	6.5	27.5	2.4	9976	776	315	2400	22	0	92	1556	4862	15.3	12.60
14	Quaternary	7.1	4	6	27.5	2.45	3849	484	116	700	11	0	79	960	1539	16.1	9.80
15	Quaternary	7.2	5.5	7	28.9	3.17	4214	458	162	780	14	0	67	1105	1662	12.4	7.00
16	Quaternary	7.2	–	–	28	3.17	2703	319	92	480	9	0	61	790	983	8.5	4.20
17	Quaternary	7.8	20	–	32.3	0.45	1111	26	9	380	9	12	195	180	397	6.7	5.60
18	Quaternary	7.4	–	–	26	2.9	2790	331	100	500	9	0	73	811	1003	9.3	8.40
19	Quaternary	7.3	–	–	30.5	2.79	2138	269	58	400	8	0	55	591	784	11.1	9.80
25	Quaternary	7.1	6	8	27.3	2.45	5631	657	140	1150	15	0	92	1141	2482	15.8	12.60
27	Quaternary	7.5	6	28	21	2.9	2117	172	64	480	14	12	140	541	765	9.1	9.80
28	Quaternary	7.6	–	–	21	1.2	427	51	24	64	16	12	244	63	74	14.1	11.20
29	Quaternary	7.1	17.5	–	27.1	0.9	4650	299	66	1300	31	0	31	835	2104	6.3	9.80
31	Quaternary	7	3	6	25.2	1	2148	249	82	360	17	0	287	830	467	25.8	12.60
32	Quaternary	7.3	6	7	24.4	1.59	849	86	39	155	9	12	183	278	179	16.5	19.60
33	Quaternary	7.2	1.9	–	22.4	2.9	1492	147	63	270	9	0	397	606	199	23.3	8.40
34	Quaternary	7.2	3.6	–	26	1.5	1030	97	52	190	8	0	305	333	199	21.8	7.00
35	Quaternary	7.2	–	–	25.2	1.59	933	80	39	200	7	0	275	230	238	19.3	4.20
36	Quaternary	7	–	–	26.5	1.9	2473	221	75	520	14	0	451	892	526	26.7	7.00
37	Quaternary	7.1	–	–	25.5	1.53	914	67	60	170	9	0	329	320	124	23.8	4.20
40	Quaternary	8.3	–	–		4.4	1607	90	66	380	8	18	79	479	526	18.9	0.00
41	Quaternary	7.3	–	–	25.6	2.6	3523	367	104	700	14	0	226	1208	1018	30.3	5.60
42	Quaternary	8.6	–	–	–	7.8	5705	598	194	1100	21	12	37	1678	2085	15.4	19.60
43	Quaternary	7.9	–	–	–	4.13	2978	289	140	540	13	18	110	830	1092	20.8	0.00
44	Quaternary	8.1	–	–	–	4.4	1586	188	58	270	12	18	146	540	427	6.3	2.80
45	Quaternary	7.3	–	–	25.1	2.6	2280	159	92	480	21	0	256	834	566	8.4	12.60
46	Quaternary	7.1	–	–	–	–	2170	326	90	260	7	0	120	888	539	9.3	
47	Quaternary	7.3					1485	175	42	256	5	0	72	650	322	10.3	
1	P-Nubian	7.1	76	–	25	3.54	6969	438	242	1700	18	0	85	1450	3078	14.7	8.40
2	P-Nubian	7.1	30	72	24.2	1.91	5871	528	194	1300	31	0	116	1227	2534	12.5	33.60
3	P-Nubian	7.1	70	125	30.1	1.8	5649	518	179	1250	23	0	92	1200	2433	12.2	12.60
6	P-Nubian	7.2	51	95	29.1	1.82	6707	319	266	1700	29	0	140	1490	2833	11.3	11.20
10	P-Nubian	7.2	40	110	29.7	3.31	4152	418	133	860	15	0	73	1051	1638	13.6	5.60
20	P-Nubian	7.2	48	160	29.9	1.3	1299	147	31	260	7	0	92	361	447	12.9	9.80
21	P-Nubian	7.1	50	200	24.2	3.1	1478	183	36	300	10	0	85	300	606	9.8	8.40
22	P-Nubian	8	60	170	22.9	3.9	1353	157	41	270	10	6	61	361	477	11.4	4.20
23	P-Nubian	6.7	28	115	28.1	1.59	1339	78	32	350	7	0	79	356	477	7.9	5.60
26	P-Nubian	7.4	35	75	–	2.83	4546	462	145	950	17	0	67	1151	1787	11.5	4.20
38	P-Nubian	8.1	47	90	–	–	1134	88	59	210	13	12	104	475	226	15.7	2.80
39	P-Nubian	7.6	40	70	26.8	3	4624	345	175	1050	16	0	92	1106	1887	15.5	16.80
4	Nubian	7.6	Flowing	800	44.4	0	1663	30	10	590	8	12	203	206	706	9.6	8.40
8	Nubian	8.2	Flowing	650	35.6	0	1737	31	11	610	19	18	165	141	826	9.5	8.40
24	Nubian	7.9	2	620	40	3	1676	92	27	470	21	12	116	430	566	9.0	7.00
30	Surface (Nile)	7.9	5		21.5	2.7	182	26	11	20	7	6	104	46	15	4.1	5.60
48	Canal Water	8	–	–	–	–	1350	87	62	335	4	5	223	406	417	6.3	–

Note: DTW is depth to groundwater level (m); TD is total depth of groundwater well (m); DO is dissolved oxygen; and Canal Water refers to a surface water sample collected from a subchannel from the River Nile.

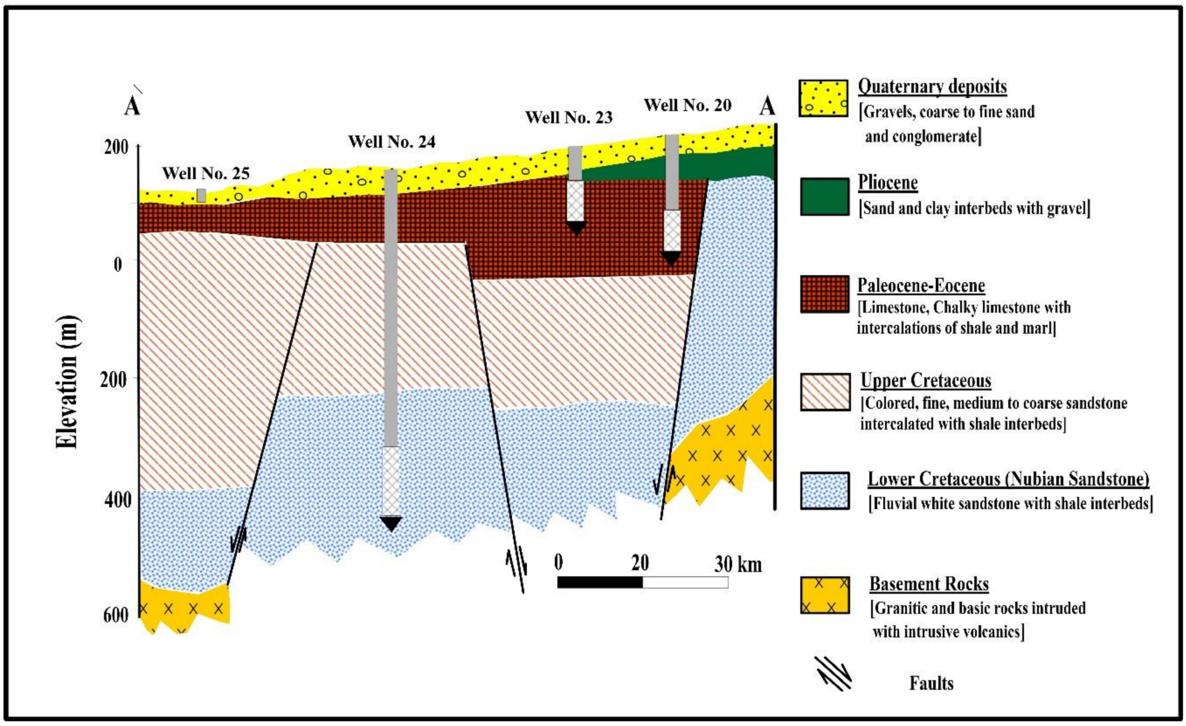

Figure 3. N-S hydrogeological cross-section along traverse A-A' of Figure 1, based on subsurface lithological data modified from [24,37].

3. Methodology

Water samples were collected from 48 wells (Table 1) in November 2018; Figure 1 shows the well location map of the study area. Samples were collected in polyethylene bottles for geochemical and isotopic analyses. pH and electrical conductivity (EC) were measured in the field. Electrical conductivity was measured using AD-410 ADWA testers; pH was measured using the AD-11 ADWA model; testers were calibrated twice daily during the field campaign. Dissolved major-ion analyses, including anions (Cl, SO_4, and HCO_3) and cations (Ca, Mg, Na, and K), were conducted at the Desert Research Center, Water Central Laboratory, Cairo, Egypt. Total dissolved solids (TDS) were estimated using the calculation method. Major cations and anions were analyzed in groundwater samples according to [39,40]. Carbonate ($CO_3{}^{2-}$) and bicarbonate ($HCO_3{}^{-}$) levels were determined via titration against H_2SO_4 using the neutralization method, using phenolphthalein as an indicator for $CO_3{}^{2-}$ and methyl orange as an indicator for $HCO_3{}^{-}$. Chloride (Cl^-) levels were determined volumetrically via titration against $AgNO_3$ using K_2CrO_4 as an indicator. Calcium (Ca^{2+}) and magnesium (Mg^{2+}) levels were determined via titration against Na_2EDTA using a complex metric method. Calcium levels were determined using a murexide indicator; magnesium levels were estimated by subtracting the calcium values from the (Ca^{2+} + Mg^{2+}) values after determining them using Eriochrome Black T in the presence of a suitable buffer solution. A Flame Photometer (PFP 7, Jenway, London, UK) was used to determine sodium (Na^+) and potassium (K^+) levels. Sulfate ($SO_4{}^{2-}$) levels were determined using the turbidity method using a UV/Visible Spectrophotometer, Unicam UV 300 (Thermo Spectronic, Waltham, MA, USA). The calculated e Error% $= [\sum \text{Cations} - \sum \text{Anions}]/[\sum \text{Cations} + \sum \text{Anions}]$ was less than 5%.

Stable isotopic analyses for $\delta^{18}O$ and $\delta^{2}H$ were analyzed at the Stable Isotope and Radiocarbon Units, Institute of Nanoscience and Nanotechnology (INN), National Centre for Scientific Research "Demokritos" on a continuous flow Finnigan DELTA V plus equipped with a Gas bench device (Thermo Electron Corporation, Bremen, Germany) stable isotope mass spectrometer. Results are expressed in the standard notation, delta per mil (δ‰), for both Oxygen ($\delta^{18}O$) and deuterium ($\delta^{2}H$).

Data obtained from the chemical analyses were used as input data for NETPATHXL [41] inverse geochemical modeling. NETPATHXL is a computer program that uses inverse geochemical modeling techniques to calculate net geochemical reactions that can account for changes in water chemistry between initial and final evolutionary waters along the flow path [15,42].

4. Results

4.1. Groundwater Chemistry

The chemical characteristics of the groundwater in the studied aquifers are presented in Table 1. According to the results of the chemical analyses, the pH of Quaternary aquifer groundwater ranged from 6.8 to 8.6 with a median of 7.3, the pH of PNA samples ranged from 6.7 to 8.1 with a median of 7.2, and the pH of NSA samples ranged from 7.6 to 8.2 with a median of 7.9. The pH values reflect that most groundwater samples had neutral to slightly alkaline characteristics. Groundwater temperature mainly depends on the geothermal gradient and ambient temperature at the land surface [43]. The groundwater temperature in the Quaternary aquifer ranged from 21 to 32.3 °C, the PNA samples' temperatures ranged from 22.9 °C to 30.1 °C, and the NSA samples' temperatures ranged from 35.6 °C to 44.4 °C (Figure 4a). The total dissolved solids (TDS) measurement is usually used as a general indicator of water quality [44]. Groundwater is classified as a fresh, brackish, and saline [45]. Results (Table 1) show that the Quaternary groundwater's TDS measurements ranged from 426 to 9975 mg/L with a median value of 2472.6 mg/L, identifying it as a fresh to saline water type. The PNA samples' TDS measurements ranged from 1134 to 6969 mg/L with a median of 4348.9 mg/L, identifying it as a fresh to saline water type. The NSA samples' TDS measurements ranged from 1496 to 1737 mg/L with a median value of 1676 mg/L, identifying it as brackish water (Figure 4b). In the upper region of the analyzed area the Quaternary and PNA groundwater had lower TDS values (Figure 1) which may be attributed to the direct recharge from local precipitation. In addition, the Quaternary groundwater downward, close to the River Nile, had lower TDS values, indicating that the River Nile percolates into the aquifer. In general, most of the major ions (Na^{+}, Mg^{2+}, Ca^{2+}, $SO_4{}^{2-}$, and Cl^{-}) were positively correlated with TDS (Figure 5a–f), indicating that their concentrations' increase was controlled by flow path, geochemical processes, and water–rock interaction between the groundwater and aquifer matrix.

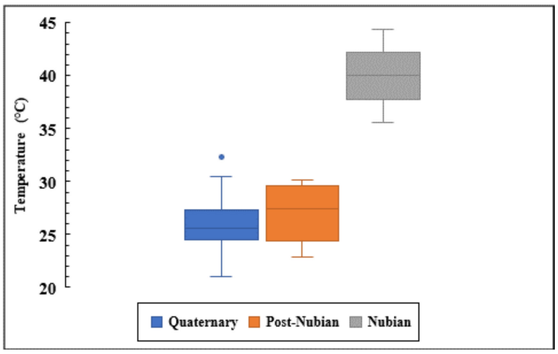

(a)

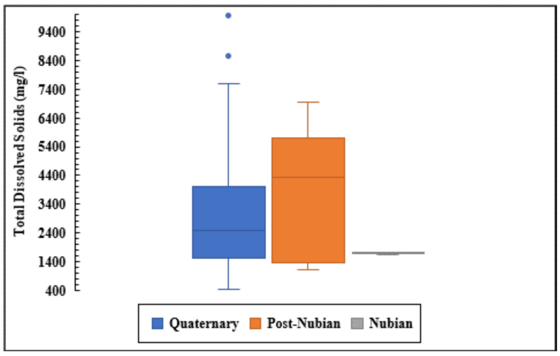

(b)

Figure 4. Box plot for the (**a**) temperature (°C) and (**b**) TDS (mg/L) of groundwater in the Wadi Qena basin.

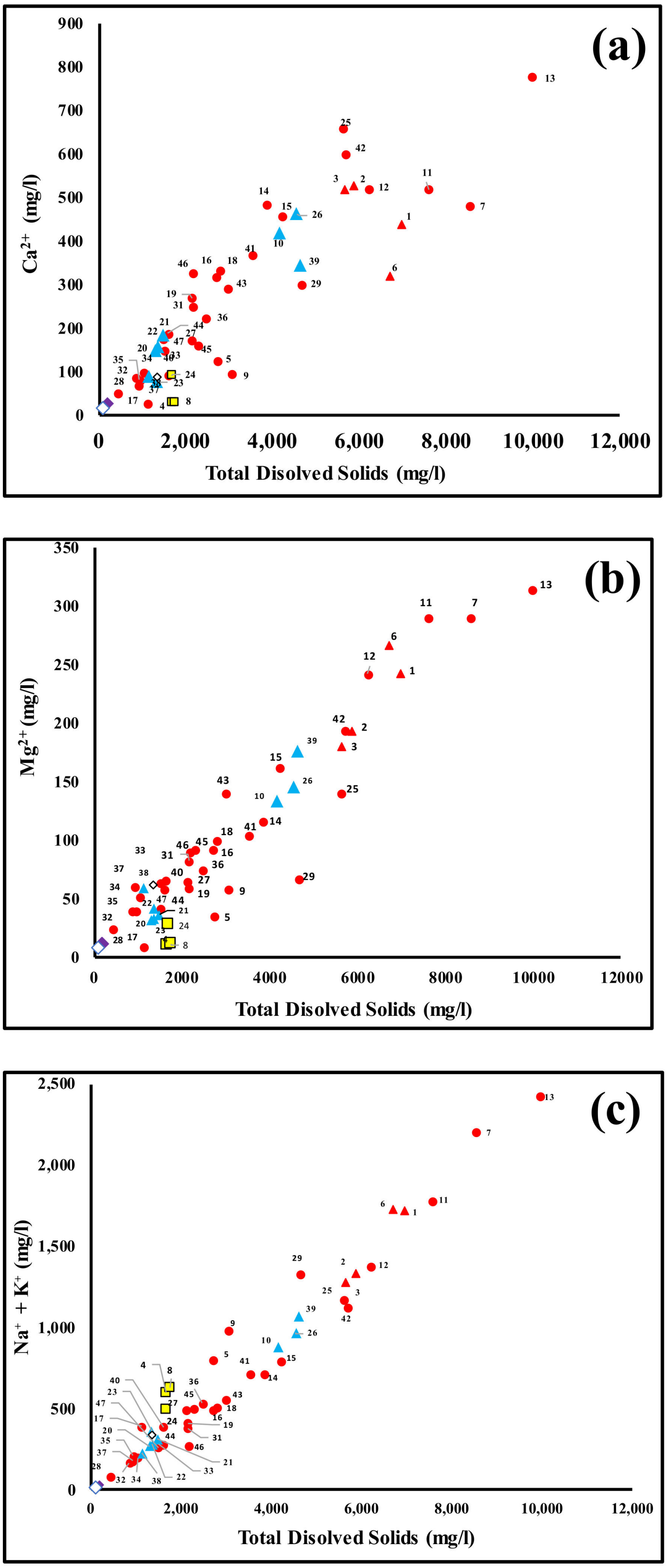

Figure 5. *Cont.*

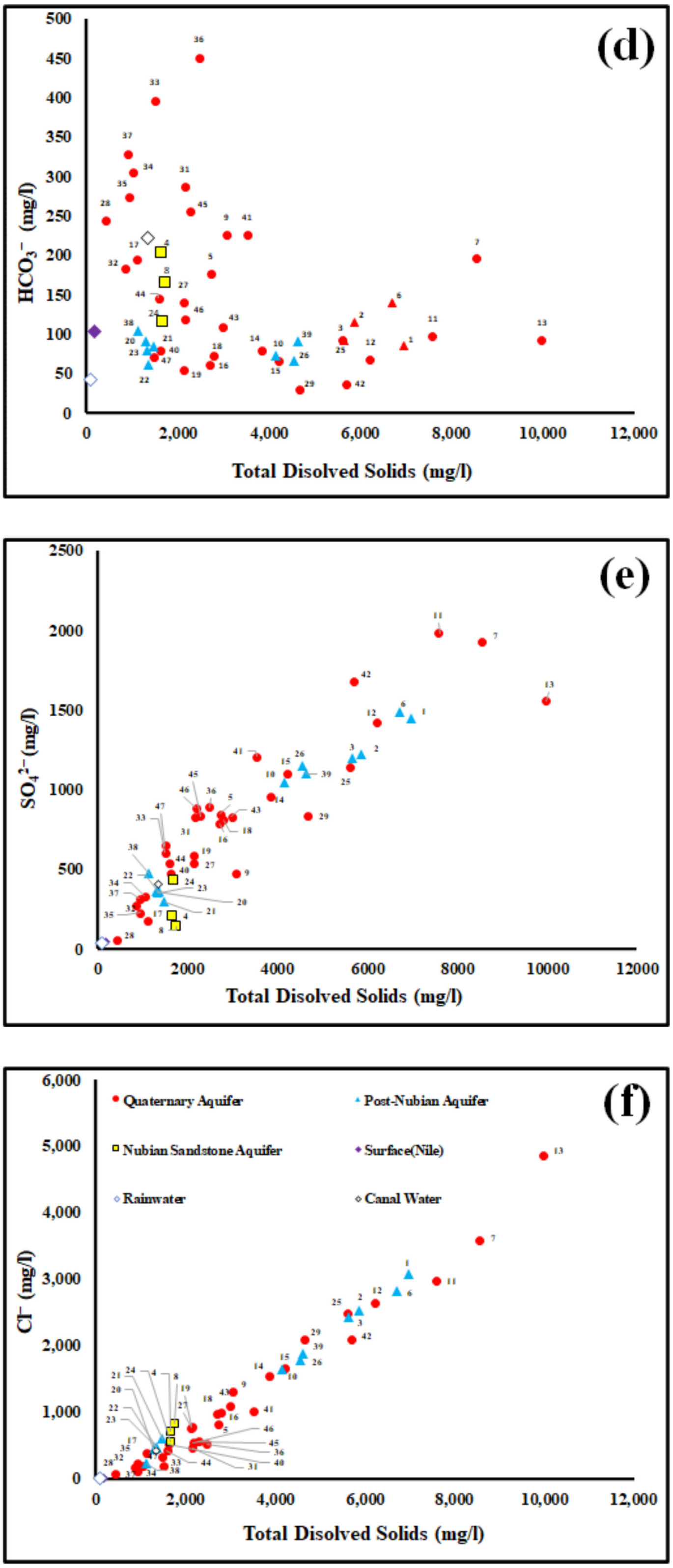

Figure 5. Major ions concentrations (mg/L) versus total dissolved solids (TDS) in mg/L relationships for groundwater wells tapping aquifers in the Qena basin (**a**) Ca^{2+} Versus TDS, (**b**) Mg^{2+} versus TDS, (**c**) Na^{+}+K^{+} versus TDS, (**d**) HCO_3^{-} versus TDS, (**e**) Cl^{-} versus TDS, and (**f**) SO_4^{2-} versus TDS.

4.2. Chemical Water Types

The major ion chemistry is shown by Piper's tri-linear diagram (Figure 6; [46]), which provides information regarding hydrogeochemical facies and the evolution of groundwater based on the relative proportions of major ions [47]. In the lower left triangle of the Piper diagram, groundwater samples from different aquifers are plotted between the two end members of the NSA groundwater and the surface water (Nile water and canal water). In the lower right triangle, groundwater samples from the NSA and PNA are shown to have higher Cl contents. In the diamond diagram, most of the three aquifer groundwater samples are distributed in subareas 7 and 9. Approximately 52% of the Quaternary groundwater samples, 100% of the PNA and NSA groundwater samples, and all canal samples are plotted in subarea 7, reflecting that Na and Ca are dominant cations, and that Cl and SO_4 are dominant anions. In subarea 7, PNA samples are plotted in the upper corner of the diamond; NSA samples are plotted in the right side corner, due to variations in groundwater chemistry as a result of leaching and dissolution of diverse minerals rich in chloride that are embedded and form different aquifer matrices. In contrast, 32.26% of Quaternary groundwater samples are in subarea (9), where no cation–anion pair exceeds 50%, reflecting the impact of the mixing process due to drainage water infiltration.

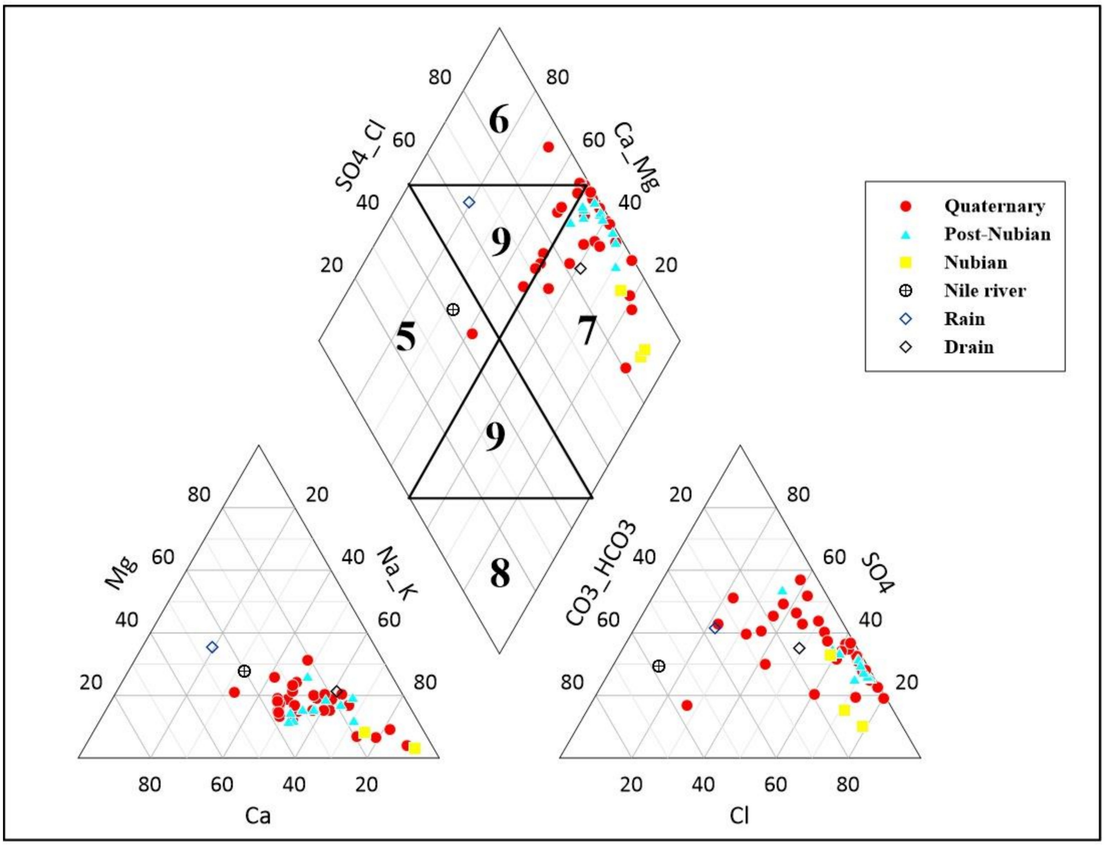

Figure 6. Piper diagram [46] showing the major ion water types of all water samples. Chemistry of the rainwater sample [48].

4.3. Environmental Isotopes

Oxygen $\delta^{18}O$ and hydrogen $\delta^{2}H$ are ideal tracer isotopes that can be used to determine groundwater recharge and mixing sources. They form part of a water molecule that does not contribute to geochemical reactions; therefore, they provide good insights into the physical processes affecting groundwater, such as groundwater mixing and evaporation [49,50]. Based on isotopic data from groundwater samples collected in November 2018 and other historical records [23,24,51], isotope analysis results show that Oxygen $\delta^{18}O$ in Quaternary groundwater ranged from −5.51‰ (well 54) to +4.7‰ (well 28), from −5.9 ‰ (well 26) to +4.9‰ (well 38) in PNA groundwater, and from −9 ‰ (well 4) to −4.81 ‰ (well 103) in NSA groundwater. The hydrogen δ^2H isotopes in the Quaternary aquifer ranged from −40.87 ‰ (well 54) to 37‰ (well 32), from −58‰ (well 26) to 43‰ (well 38) in the PNA, and from −71‰ (well 4) to −33.22‰ (well 93) in the NSA. The δ^{18}O–δ^2H relationship (Figure 7a and Table 2) shows that most groundwater samples fell close to the global meteoric water line (GMWL, [52]), indicating that they were mainly of meteoric origin.

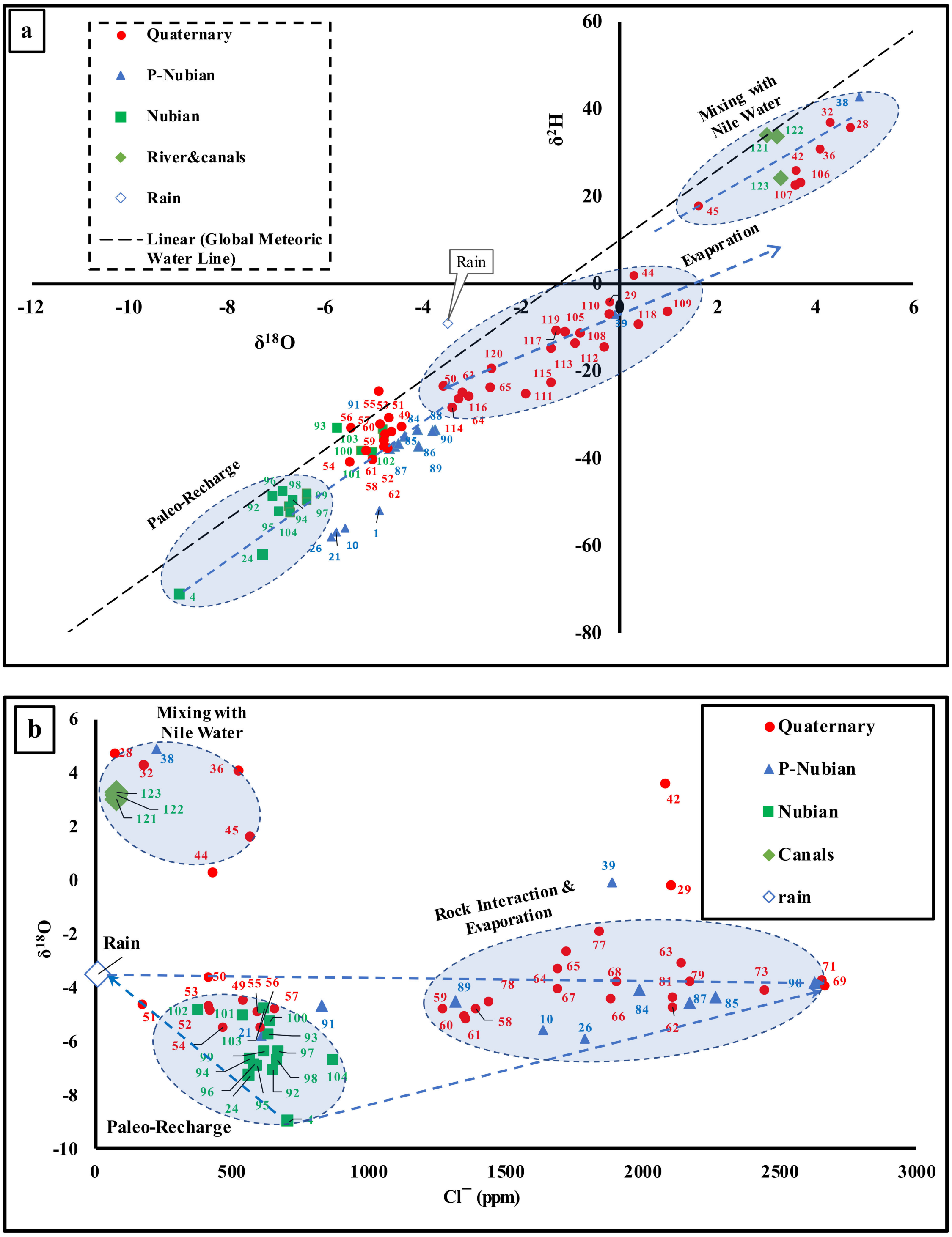

Figure 7. (**a**) δ^{18}O (‰) versus δ^2H (‰) and Cl^- (mg/L) (**b**) δ^{18}O (‰) versus Cl (mg/L) for groundwater samples tapping different aquifers in the Qena Basin, (GMWL, from [51]). Isotopic data serials greater than 48 are from [23,24,51]; the rainwater sample is from [53].

Table 2. Recent and historical isotopic record data for chloride concentration (ppm), $\delta^{18}O$ (‰), and $\delta^{2}H$ (‰).

No.	Aquifer	Cl	$\delta^{18}O$	$\delta^{2}H$	No.	Aquifer	Cl	$\delta^{18}O$	$\delta^{2}H$	No.	Aquifer	Cl	$\delta^{18}O$	$\delta^{2}H$
		ppm	(‰)				ppm	(‰)	(‰)			ppm	(‰)	
28 *	Quaternary	74	4.7	36	64	Quaternary	1692	−3.27	−26.36	94	Nubian	566	−6.66	−49.59
29 *	Quaternary	2104	−0.2	−4	65	Quaternary	1719	−2.64	−23.86	95	Nubian	590	−6.95	−52.33
32 *	Quaternary	179	4.3	37	66	Quaternary	1859	−4.44	−34.81	96	Nubian	580	−6.87	−47.65
36 *	Quaternary	526	4.1	31	67	Quaternary	1689	−4.04	−34.74	97	Nubian	669	−6.39	−49.74
42 *	Quaternary	2085	3.6	26	68	Quaternary	1902	−3.79	−34.19	98	Nubian	665	−6.74	−50.92
44 *	Quaternary	427	0.3	2	69	Quaternary	2667	−3.92	−33.36	99	Nubian	617	−6.39	−48.21
45 *	Quaternary	566	1.6	18	70	Quaternary	3407	−2.73	−29.55	100	Nubian	640	−5.26	−38.17
1 *	P-Nubian	3078	−4.9	−52	71	Quaternary	2654	−3.72	−32.79	101	Nubian	541	−5.05	−38.54
10 *	P-Nubian	1638	−5.6	−56	72	Quaternary	8783	−2.06	−27.52	102	Nubian	377	−4.82	−33.28
21 *	P-Nubian	606	−5.8	−57	73	Quaternary	2445	−4.08	−33.49	103	Nubian	621	−4.81	−35.24
26 *	P-Nubian	1787	−5.9	−58	74	Quaternary	5355	−0.58	−19.59	104	Nubian	869	−6.72	−52.46
38 *	P-Nubian	226	4.9	43	75	Quaternary	4845	−3.43	−32.88	105	Quaternary	655	−0.8	−11.2
39 *	P-Nubian	1887	−0.1	−7	76	Quaternary	4095	−3.04	−30.07	106	Quaternary	50	3.7	23.3
4 *	Nubian	706	−9	−71	77	Quaternary	1844	−1.89	−30.24	107	Quaternary	46	3.6	22.5
24 *	Nubian	566	−7.3	−62	78	Quaternary	1437	−4.55	−38.68	108	Quaternary	822	−0.3	−14.4
49	Quaternary	541	−4.45	−32.73	79	Quaternary	2173	−3.8	−32.61	109	Quaternary	1287	1	−6.5
50	Quaternary	412	−3.6	−23.5	80	Quaternary	3132	−4.02	−34.55	110	Quaternary	851	−0.2	−6.9
51	Quaternary	173	−4.64	−33.85	81	Quaternary	2109	−4.34	−35.97	111	Quaternary	1158	−1.9	−25.3
52	Quaternary	420	−4.87	−32.34	82	Quaternary	3481	−4.26	−37.78	112	Quaternary	1280	−0.9	−13.7
53	Quaternary	413	−4.69	−30.87	83	Quaternary	3807	−1.4	−25.22	113	Quaternary	2580	−1.4	−14.8
54	Quaternary	464	−5.51	−40.87	84	P-Nubian	1988	−4.12	−33.34	114	Quaternary	601	−3.4	−28.4
55	Quaternary	592	−4.9	−24.78	85	P-Nubian	2269	−4.38	−34.82	115	Quaternary	531	−1.4	−22.5
56	Quaternary	605	−5.48	−33.15	86	P-Nubian	3279	−4.11	−37.11	116	Quaternary	1230	−3.2	−25.1
57	Quaternary	654	−4.79	−34.46	87	P-Nubian	2175	−4.6	−37.22	117	Quaternary	385	−1.3	−10.8
58	Quaternary	1390	−4.81	−37.3	88	P-Nubian	5323	−3.78	−33.37	118	Quaternary	525	0.4	−9.2
59	Quaternary	1268	−4.81	−35.95	89	P-Nubian	1318	−4.51	−36.67	119	Quaternary	1300	−1.1	−11.1
60	Quaternary	1355	−5.16	−38.27	90	P-Nubian	2632	−3.81	−33.7	120	Quaternary	616	−2.6	−19.5
61	Quaternary	1348	−5.05	−40.28	91	P-Nubian	826	−4.69	−37.72	121	Canal Water	80	3	34.1
62	Quaternary	2110	−4.72	−37.63	92	Nubian	648	−7.07	−48.67	122	Canal Water	80	3.2	34
63	Quaternary	2142	−3.08	−25.89	93	Nubian	636	−5.77	−33.22	123	Canal Water	80	3.3	24.3

Note: Isotopic data marked with an asterisk (*) are samples collected in November 2018; other data are from [23,24,51]. Canal Water refers to a surface water sample collected from a subchannel from the River Nile.

5. Discussion

The current study attempts to utilize geochemical and environmental isotopic tracers to understand the geochemistry of groundwater and recharge sources to determine evolutionary processes in the Qena Basin, Eastern Nile Valley, Egypt. Integrating isotopic tracers with conventional hydrogeological methods can lead to relevant information regarding the origin of groundwater mineralization [16].

5.1. Geochemical Processes Affecting Groundwater

The results above show that most of the major ions (Na^{+}, Mg^{2+}, Ca^{2+}, SO_4^{2-}, and Cl^{-}) directly correlated with TDS (Figure 5a–f), indicating that increases in their concentrations were consistent with the flow path from upstream (northeast) to downstream (southwest) (Figure 1). Both geochemical and physical processes (dissolution and evaporation) as well as water–rock interaction were controlling factors for salinity variations in the study area (Figure 8; [54]). Figure 8 represents the ratios of $((Na^{+} + K^{+})/Na^{+} + K^{+} + Ca^{+2})$ and major anions $(Cl^{-}/Cl^{-} + HCO_3^{-})$ separately, as a function of TDS. The plot indicates that groundwater samples of the studied aquifers were primarily distributed in the evaporation dominance field. This suggests that the groundwater chemistry in the area was primarily controlled by the evaporation process, as well as the water–rock interaction factor, because the annual rainfall and groundwater recharge were insignificant.

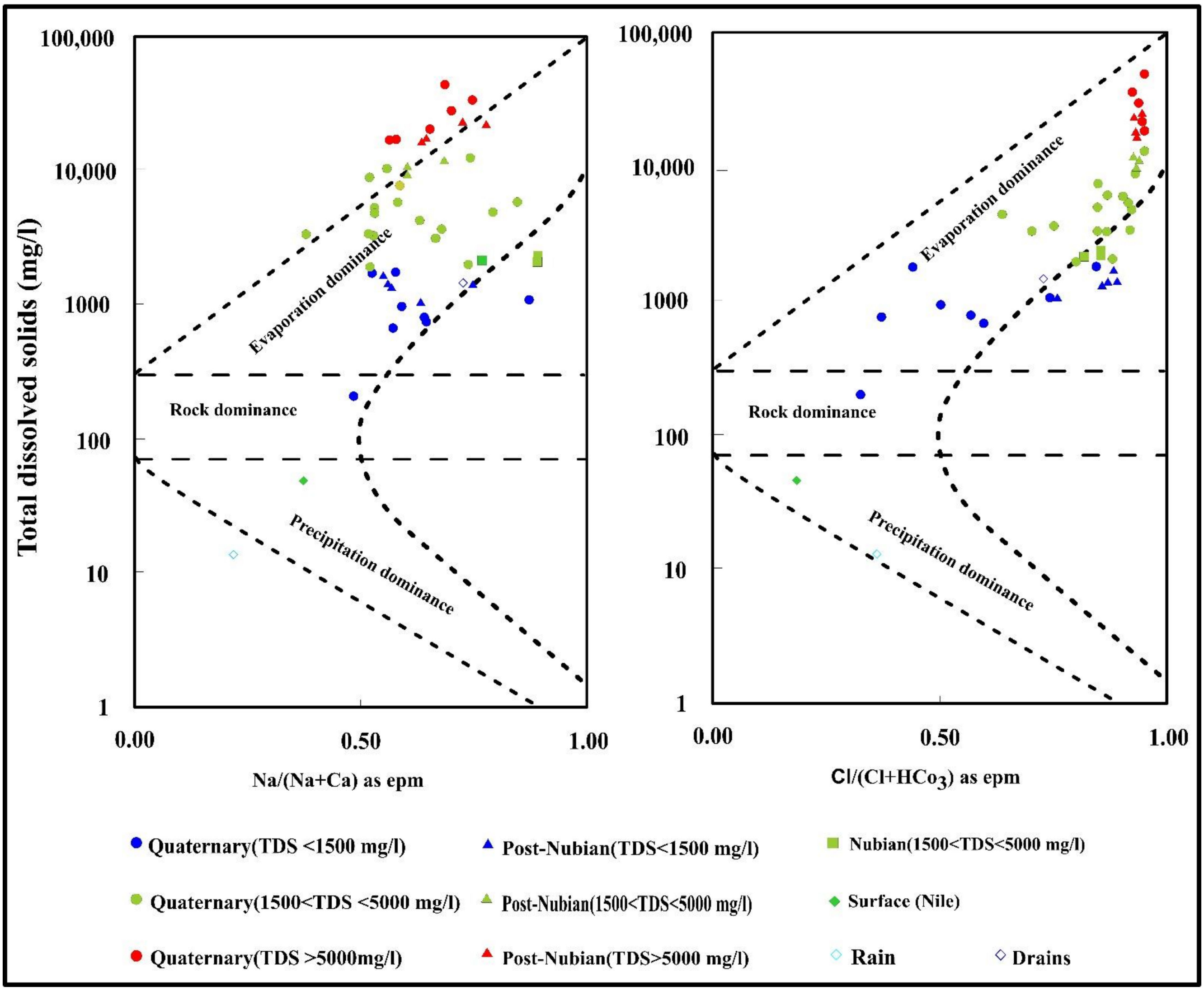

Figure 8. Gibbs's diagram with all water samples represents ratios of Na/(Na + Ca) and Cl/(Cl + HCO_3) as a function of TDS. The chemistry of the rainwater sample is from [48].

The influence of hydrochemical processes that affect water quality such as ion exchange, mixing, and leaching can be detected using chemical ion ratios [55–57]. In the current study, the relations between different ionic concentrations were used to understand the relationships between the ions and factors affecting groundwater chemistry (Figure 9). A higher concentration of sodium in the groundwater of the NSA and a lower concentration in the groundwater of the PNA indicate silicate weathering [58]. In contrast, the groundwater in the Quaternary aquifer and in most of the PNA samples showed a slightly lower concentration of Na^+, which may be attributed to the Ca/Na exchange process (Figure 9a) due to the presence of clay interbeds in the aquifers. The relations of Ca^{+2}/Na^+ versus $HCO_3{}^-$/Na (Figure 9b) show that most of the groundwater samples of the three aquifers had more Na^+ than Ca^{+2}, Mg^{+2}, and $HCO_3{}^-$, which could be explained by silicate weathering. The relation of ($Cl^- - Na^+$)/Cl^- vs. TDS (Figure 9c) shows that 51.61% of Quaternary samples and 83.33% of Post-Nubian samples in the study area had a positive value; this indicates a direct cation exchange process between Na^+ and K^+ dissolved in groundwater with Ca^{2+} and Mg^{2+} embedded in the aquifer matrix. In contrast, the rest of the Quaternary samples, the Post-Nubian samples and all Nubian groundwater samples had negative values that indicate a reverse cation exchange process.

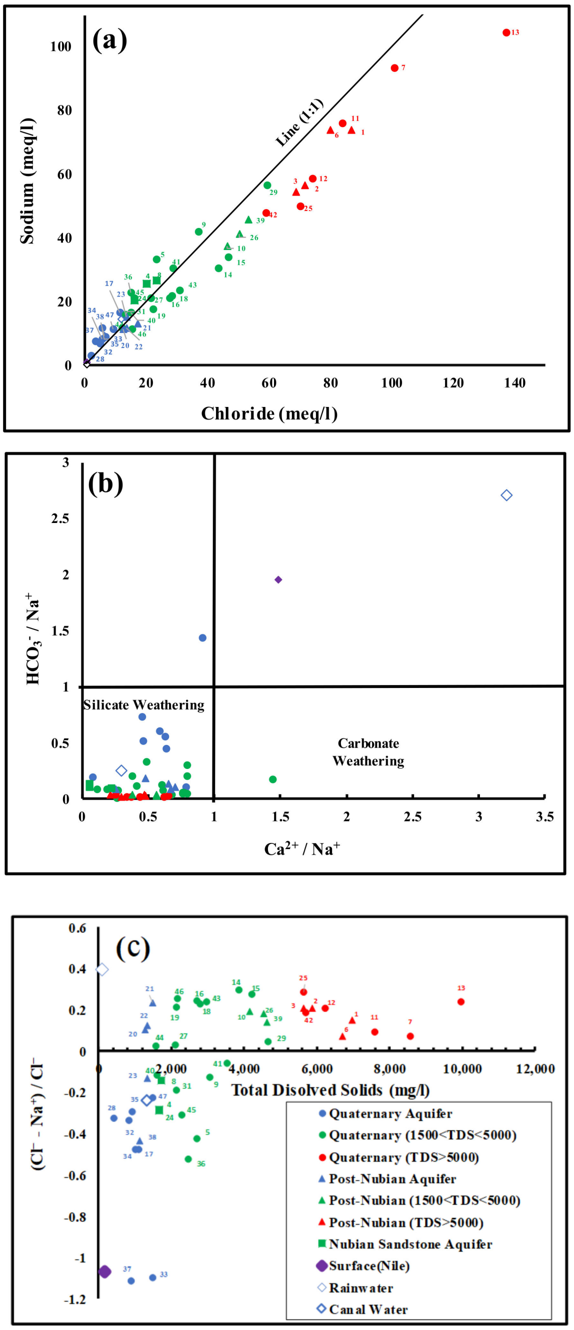

Figure 9. (**a**) $Cl^{-}Na$, (**b**) HCO_3/Na versus Ca/Na, and (**c**) TDS/$(Cl^{-}Na)/Cl$ relationships. Plots show different ionic relationships for groundwater wells tapping the three aquifers in the Qena basin.

5.2. Groundwater Recharge Mechanism

The hydrogeologic setting in the study area indicates that groundwater within the studied aquifers is generally flowing from the northeast to the southwest [5,25]. Moreover, extensive structural deformation by dextral faults trending northeast to southwest and northwest to southeast controls the water-bearing horizons in the subsurface [23,24]. Data for the stable isotopes Oxygen $\delta^{18}O$ and hydrogen $\delta^{2}H$ indicate that groundwaters from the different aquifers were primarily of meteoric origin (Figure 7a). Upstream Quaternary groundwater samples were relatively enriched with isotopic content and plotted close to the recent rainwater and the canal samples, confirming recharge from recent meteoric precipitation. Downstream groundwater samples located in the delta of the Qena basin were plotted close to the canal samples, indicating mixing with current recharge from

Nile water. In contrast, NSA groundwater was relatively depleted of isotopic content compared to other groundwater samples (Quaternay and PNA) and the recent rainfall isotopic signature, which confirms a paleo-water that had been recharged in a cooler climate. The Post-Nubian groundwater samples were plotted between the Nubian and the upstream Quaternary groundwater samples. Post-Nubian aquifer groundwater originated primarily from the upward leakage from the NSA under artesian conditions and seepage from the upper unconfined Quaternary aquifer. Moreover, the relationship between $\delta^{18}O$ and Cl (Figure 7b, Table 2) shows that upstream Quaternary groundwater samples were plotted between the most depleted Nubian groundwater samples, represented by well site 4 and the rainwater sample, indicating mixing due to percolation from the QA and upward infiltration from the NSA. Downstream Quaternary groundwaters were plotted close to the canal water, indicating promising recharge due to canal water seepage. Post-Nubian and Quaternary groundwater samples plotted on the right side had high dissolved chloride concentrations, probably due to leaching and dissolution of the aquifer matrix and evaporation processes.

5.3. Water–Rock Interaction and Mixing Model

Chemical data from the groundwater samples and isotopic data were used in the NETPATH Model to estimate geochemical reaction and mixing with other sources [15,50]. This model estimates net geochemical reactions and observed variations in groundwater chemistry between initial and final groundwater wells along the groundwater subsurface flow path. However, this approach is limited by the input data related to the subsurface groundwater aquifer [59]. In this study, the NETPATH geochemical model is constrained by major dissolved ions in the groundwater including carbon (carbonate and bicarbonate ions) sulfur (to represent sulfate anions), calcium, magnesium, sodium, chloride, and silica (Table 3).

Table 3. Constraints, phases, and processes used in NETPATH models.

Constraints	Phases	Processes
Calcium, Carbon, Magnesium, Potassium, Sodium, Sulfur, Chloride, Silica	Albite, Alunite, Calcite, Chlorite, (±) Dolomite, (−) Ca-Montmorillonite, K-Mica, Illite, Gypsum, Sio_2, (+) Halite NaCl, (−) Anorthite, (±) Exchange	Reaction and/or Evaporation and Mixing

Note: (±) Dissolution and precipitation, (+) dissolution only, and (−) precipitation only.

The essential minerals embedded in the aquifer sediment were used as input phases to represent the interaction and hydrolysis between the groundwater and aquifer matrix. Calcite, dolomite, and halite minerals dominate terrestrial alluvial deposits (Quaternary aquifer) and the Post-Nubian carbonate aquifer. Gypsum, montmorillonite, and illite are dominant in the clay sheet intercalations of the Quaternary aquifer and the impervious Quseir variegated shale overlying the NSA [1]. Anorthite, alunite, and chlorite are used to simulate the basement aquifer and the main watershed area of the Qena basin.

The Qena watershed is in Egypt's arid zone; therefore, the evaporation parameter was selected to simulate the impact of aridity and scarce rainfall on groundwater salinization. A mixing parameter was used to simulate the possibility of recharge from the River Nile and mutual leakage from the multiple aquifer hydrologic system (confined, unconfined, and semi-confined). The model results show two main factors controlling the groundwater geochemistry: water–rock interaction and mixing models (Table 4).

Table 4. NETPATH water–rock interaction and mixing model results (mmol/L) representing groundwater in the Qena Watershed.

Model	Aquifer	Initial Water-1	Initial Water-2	Final Water	Mixing Percent		Phases Precipitated or Dissolved													
					Initial Water-1	Initial Water-2	Cal	Dol	Gyp	Hal	Si	Ilt	Chrt	Mont	Albt	An	Mic	Alun	Ex	Ev
Reaction Models	Quaternary aquifer (Upstream)	54	None	55	–	–	2.41	−1.89	0.31	4.85	6.66	–	0.35	–	−2.58	–	–	−0.01	–	–
		54	None	57	–	–	–	–	1.79	5.78	9.48	–	0.37	–	−2.69	−1.26	–		–	1.04
		54	None	58	–	–	−10.4	6.08	1.73	27.51	9.36	–		–	−3.12	–	–	−0.41	–	–
		57	None	59	–	–	3.29	–	9.64	17.44	22.83	–	0.47	–	−8.08	–	–	–	7.36	–
		59	None	66	–	–	–	−2.38	3.36	12.83	–	–	0.83	–	–	−1.25	–	–	−6.00	1.08
		66	None	71	–	–	3	−1.77	–	6.66	12.25	0.31	0.25	–	−3.99	–	–	–	–	1.27
	Post-Nubian	10	None	84	–	–	0.90	–	4.90	–	5.02	–	0.38	–	–	−3.13	–	–	3.4	1.22
		84	None	90	–	–	–	−0.16	6.79	14.89	5.32	–	–	–	−1.77	–	–	−0.07	1.02	1.05
Mixing Models	Quaternary aquifer (Upstream)	8	Rain	9	87.2	12.8	1.36	–	3.66	16.85	–	–	0.39	–	1.84	−3.39	–	–	–	–
		94	Rain	17	69.50	30.50	1.25	–	–	–	–	–	−0.24	−3.84	6.04	−1.66	–	−0.22	–	–
		95	Rain	18	21.40	78.60	–	–	7.79	24.55	22.11	–	0.69	−1.44	−6.34		–	–	–	–
		24	Rain	19	21.50	78.50	–	–	5.06	18.49	13.79	–	0.39	–	5.56	0.93	–	–	–	–
		103	Rain	51	26.5	73.5	2.54	–	4.62	–	–	–	0.10	−0.88	3.37	−3.58	–	–	–	–
		103	Rain	53	65.9	34.1	0.51	–	2.68	–	–	–	0.19	–	1.28	−2.20	–	−0.22	–	–
		101	Rain	54	77	23	−4.46	2.95	–	–	–	–	−0.72	–	5.19	–	−4.48	−0.65	–	–
	Quaternary aquifer (Down-stream)	44	Nile	28	14.5	85.5	−2.29	2.33	–	–	–	0.09	−0.42	–	0.34	–	–	−0.28	–	–
		44	Nile	32	39.7	60.3	−1.15	1.22	–	–	–		−0.17	−1.08	1.55	–	–	0.19	–	–
		44	Nile	36	41	59	−0.22	3.45	–	9.66	–	−6.48	–	–	7.67	–	–	3.36	–	–
		44	Nile	45	52	48	–	1.25	–	9.55	–		0.22	–	4.86	–	−5.11	2.78	–	–
	Post-Nubian	101	Rain	20	82	18	0.88	−0.57	–	–	2.02	–	0.02	–	−0.66	–	–	−0.46	–	–
		92	Rain	21	93.5	6.5	5.04	−3.05	–	–	8.24	–	0.47	–	−3.19	–	–	−0.06	–	–
		101	Rain	22	87.8	12.2	1.5	−1.26	–	–	–	–	0.22	0.64	−1.04	−0.61	–	–	–	–

Note: Cal = calcite; Dol = dolomite; Gyp = gypsum; Hal = halite; Si = silica; Ilt = illite; Chrt = chlorite; Mont = Ca-montmorillonite; Albt = albite; An = anorthite, Alun = alunite; Ex = exchange; Ev = evaporation factor. Well locations for initial water-1, initial water-2, and final waters are indicated in Figures 1 and 10.

The water–rock interaction models well describe the evolution and salinization processes of the Quaternary groundwater located at the upstream watershed of Wadi Qena. Geochemical water–rock interaction modeling results suggest the dissolution of calcite, gypsum, halite, silica, illite, and chlorite as groundwater flows downward; dolomite, albite, anorthite, and alunite are precipitated, and some cation exchange occurs (e.g., from initial water-1 represented by sample 54 to final water at sites 55, 57, 58; from site 57 to 59; site 59 to 66, and site 66 to 71; see Table 4 and Figure 10). The evaporation factor for groundwater in this area ranges from 1.04 to 1.2. Groundwater in the PNA evolved from site 10 (initial water-1) to site 84 (final water), and then from site 84 (initial water-1) to site 90 (final water). The model converges via the dissolution of calcite, gypsum halite, and silica; de-dolomitization; precipitation of albite and anorthite; some cation exchange; and an evaporation factor ranging from 1.05 to 1.22.

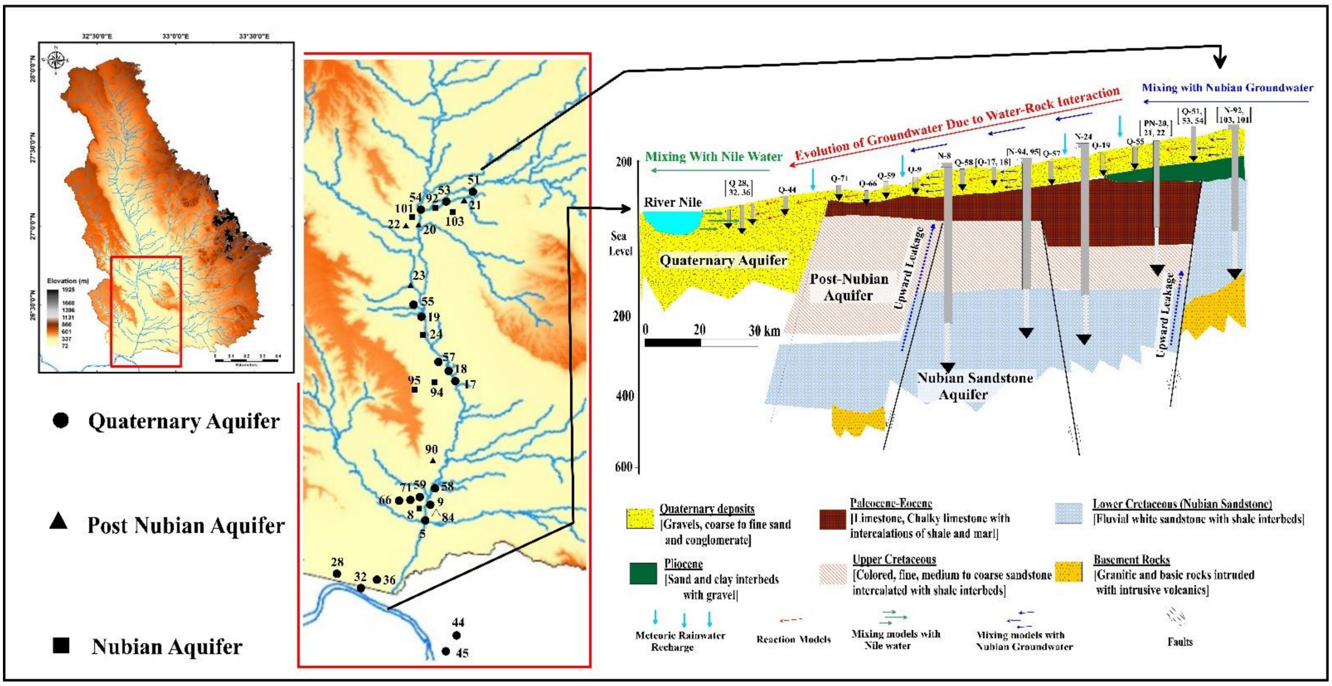

Figure 10. Schematic cross-section showing the geochemical processes controlling groundwater quality based on NETPATH geochemical model results reported in Table 4.

To simulate the recharge and mixing from Nubian groundwater toward the other two aquifers, eleven model scenarios were converged for the Quaternary aquifer and three models for the Post-Nubian aquifer. To simulate upward leakage from the NSA toward the Quaternary groundwater aquifer located upstream, Nubian groundwater sites 8, 94, 95, 24, 103, and 101 were used as initial water-1, rainwater was used as initial water-2, and Quaternary groundwater sites 9, 17, 18, 19, 51, 53, and 54 were used as final waters in the NETPATH model. Model results for the shallow Quaternary groundwater aquifer located upstream of the Qena basin close to the confined NSA primarily indicated dissolution of calcite, gypsum, dolomite, halite, chlorite, and albite, and that clay minerals (illite, Ca-montmorillonite) and alunite were formed (Table 4). The estimated mixing percentages from the Nubian toward the Quaternary groundwater ranged from 21.4 % to 87.2 %; the recharge percentages from rainwater ranged from 78.6 % to 12.8%. The mixing NETPATH model results suggest that the downstream Quaternary alluvial groundwater aquifer located in the Wadi Qena delta area is mainly recharged from canal water (River Nile branches). The calculated mixing ratio ranged from 48% from original groundwater that comes from the upstream watershed represented by site 44 (final water at site 45) to 85.5% from Nile water (final water at site 28). The calculated mixing percentage from

Nubian to Post-Nubian groundwater ranged from 82 % to 93.5 % of Nubian groundwater, whereas the rainwater amount ranged from 6.5% to 18 %. Calculated mineral saturation indices (SI; Table 5) were consistent with changes in mineral phases, where the minerals that had negative saturation indices were dissolved and indicated by positive (+ve) mass transfer values in the NETPATH model, with the exception of de-dolomitization driving the dissolution of dolomite despite over-saturated SIs [60].

Table 5. Mineral saturation indices for phases in NETPATH geochemical models.

Aquifer	Well No.	Mineral Phases											
		Cal	Dol	Gyp	Hal	Si	Ilt	Chrt	Mont	Albt	An	Mic	Alun
Quaternary	5	−0.66	−1.53	−0.86	−4.86	−0.96	6.12	−5.48	6.90	0.88	0.26	13.93	6.92
	9	0.34	0.79	−1.21	−4.56	−0.99	5.05	3.60	5.07	0.99	0.26	12.05	0.66
	17	0.00	−0.05	−1.92	−5.43	−1.30	2.63	0.96	2.86	−0.64	−0.87	9.48	−1.97
	18	0.01	−0.15	−0.53	−4.97	−2.77	−1.26	−3.28	−0.96	−4.76	−2.83	6.60	2.30
	19	−0.19	−0.66	−0.67	−5.16	−1.06	4.30	0.86	5.00	0.10	0.49	11.27	1.86
	28	0.13	0.25	−1.96	−6.89	−0.89	5.81	1.19	6.12	0.28	0.49	12.99	0.82
	32	−0.12	−0.24	−1.25	−6.16	−0.84	5.78	0.08	6.47	0.63	0.64	12.91	2.78
	36	0.23	0.34	−0.63	−5.23	−0.65	6.63	−0.81	7.50	1.59	1.18	13.83	4.94
	44	0.76	1.31	−0.78	−5.57	−2.74	−1.37	0.66	−1.65	−4.70	−2.84	6.20	−0.89
	45	0.14	0.38	−0.77	−5.22	−2.76	−0.81	−4.43	−0.68	−4.72	−3.12	7.31	3.60
	51	−0.54	−1.74	−0.84	−6.08	−1.05	5.83	−7.79	7.27	0.27	0.32	13.59	6.82
	53	−0.09	−0.53	−0.26	−5.48	−1.04	6.08	−2.46	7.01	1.04	0.78	13.66	6.39
	54	0.18	0.19	−1.36	−5.43	−1.05	4.95	1.17	5.42	0.63	0.17	11.98	0.84
	55	−0.88	−2.14	−1.18	−5.21	−1.05	5.85	−6.41	7.10	0.63	0.21	13.55	6.02
	57	−0.71	−1.26	−1.12	−5.15	−1.05	6.10	−4.08	7.08	0.66	0.12	13.77	6.51
	58	0.04	−0.03	−0.32	−4.58	−1.04	6.08	−2.07	6.99	0.94	0.63	13.62	6.53
	58	−0.17	−0.47	−0.41	−4.58	−1.04	6.14	−4.39	7.25	0.93	0.42	13.81	7.57
	71	−0.14	−58.00	0.23	−4.13	−1.03	6.31	−1.85	7.03	1.15	0.86	13.98	7.09
	60	0.32	0.58	0.30	−4.50	−1.04	6.13	−2.12	3.45	1.03	0.57	13.71	6.78
	66	−0.21	−0.65	−0.10	−4.39	−1.04	6.33	−2.04	7.00	1.02	0.76	2.04	7.05
Post-Nubian	10	−0.10	−0.31	−0.43	−4.55	−0.96	5.03	1.57	5.63	0.73	0.76	12.06	3.06
	20	−0.26	−0.80	−1.00	−5.56	−0.99	4.65	−0.85	5.51	0.17	0.45	11.71	2.29
	21	−0.37	−1.11	−1.00	−5.37	−0.96	5.57	−2.26	6.45	0.53	0.65	12.94	3.87
	22	0.28	0.30	−0.97	−5.51	−2.75	−1.55	−0.37	−1.72	−4.81	−2.93	6.04	−0.99
	23	−1.12	−2.24	−1.25	−5.40	−1.19	4.62	−5.85	5.80	−0.29	−0.33	12.20	5.50
	26	−0.03	−0.26	−0.36	−4.46	−0.96	5.76	1.77	6.23	1.12	0.91	12.96	3.64
	90	−0.10	−0.47	−0.10	−4.09	−1.03	6.33	1.88	7.02	1.19	0.80	14.01	7.21
	84	−0.14	−0.58	0.03	−4.32	−1.03	6.31	−1.85	7.03	1.15	0.86	13.98	7.09
Nubian aquifer	4	−0.02	−0.01	−1.88	−5.03	−1.24	1.85	1.70	2.20	−0.73	−0.89	8.43	−2.91
	8	0.39	0.79	−2.03	−4.94	−1.18	2.39	5.49	2.11	−0.24	−0.65	8.86	−5.00
	24	0.42	0.76	−1.16	−5.22	−1.23	2.25	5.24	2.13	−0.67	−0.38	8.79	−3.02
	94	−0.67	−1.32	−1.24	−5.33	−1.05	6.01	−3.74	6.95	0.55	0.21	13.64	5.66
	95	−0.56	−1.13	−1.36	−5.28	−1.05	5.89	−3.85	6.95	0.59	0.22	13.46	5.24
	92	−0.57	−1.17	−1.17	−5.21	−1.05	6.02	−3.61	6.95	0.61	0.28	13.66	5.68
	101	−0.54	−1.33	−0.83	−5.37	−1.05	6.07	−4.02	6.97	0.53	0.41	13.78	6.20
	103	−1.31	−3.00	−2.63	−5.16	−1.05	5.84	−8.93	6.85	0.67	−0.43	13.79	4.34
Rain	Rain	−1.25	−2.53	−2.87	−8.85	−2.71	−1.13	−7.88	−0.05	−6.20	−3.57	6.65	−0.35
Nile	Nile	−0.15	−0.37	−2.25	−8.07	−2.74	−1.35	−3.30	−1.34	−5.78	−3.42	6.44	−1.52

Note: Cal = calcite; Dol = dolomite; Gyp = gypsum; Hal = halite; Si = silica; Ilt = illite; Chrt = chlorite; Mont = Ca-montmorillonite; Albt = albite; An = anorthite; Alun = alunite; Ex = exchange; and Ev = evaporation factor. Well locations for initial water-1, initial water-2, and final waters are indicated in Figures 1 and 10.

6. Conclusions

The current study utilized hydrogeochemistry and environmentally stable isotopes to determine the main recharge sources and geochemical processes affecting groundwater in the Qena basin, located in the Eastern desert of Egypt. This basin comprises three main groundwater aquifers: the Quaternary aquifer, the Post Nubian aquifer (PNA), and the Nubian Sandstone aquifer (NSA), which is mainly controlled by lithological and structural features. Groundwaters in the upstream watershed generally had fresh to brackish water, whereas those downstream were mainly brackish to saline. Isotopic data ($\delta^{18}O$ and $\delta^{2}H$) revealed that Nubian groundwater was relatively depleted, primarily of meteoric origin and a paleo-water recharged in a cooler climate. The NSA had higher groundwater temperatures than the other aquifers. Quaternary groundwater located at the upstream watershed received considerable recharge from recent meteoric water and upward leakage from the NSA. The downstream Quaternary aquifer in the delta of the Qena basin was characterized by mixed groundwater composed of upstream water with recent River Nile water. Isotopic analysis confirmed recharge of the Post-Nubian groundwater aquifer mainly from upward leakage from the NSA under artesian conditions and seepage from the upper unconfined Quaternary aquifer. NETPATH geochemical model results indicated that the evaporation process, water–rock interaction, and mixing are the physical and geochemical processes controlling groundwater quality, where leaching and dissolution processes of terrestrial minerals and silicate weathering prevail. The Nubian groundwater aquifer has a great expanse, considerable thickness, possesses good groundwater quality, and should be well explored and well managed for sustainable groundwater use.

Author Contributions: A.R.: Carried out the fieldwork and chemical analysis and field data interpretation for the geochemical groundwater characteristics. M.E.: Carried out the fieldwork, conceived of the presented idea, and write the part of the methodology, as well as interpretation of geochemical and isotopic data and contribute in writing the whole manuscript with input from all authors. I.E.S.: revise the whole manuscript and propose the research point, E.D.: Carried out measurements for stable environmental isotopes at her laboratory. M.S.: Carried out the interpretation of geochemical analyses for surface and groundwater samples. and S.M.: Shared with writing the part on groundwater geochemistry, in addition, she wrote part of the result and discussion in the manuscript. All authors have read and agreed to the published version of the manuscript.

Funding: This research received no external funding.

Institutional Review Board Statement: Not applicable.

Informed Consent Statement: Not applicable.

Data Availability Statement: Not applicable.

Conflicts of Interest: The authors declare no conflict of interest.

References

1. Said, R. *The Geology of Egypt*; Elsevier: Amesterdam, The Netherlands, 1962; p. 377.
2. Abdel-Fattah, M.; Saber, M.; Kantoush, S.A.; Khalil, M.F.; Sumi, T.; Sefelnasr, A.M. A hydrological and geomorphometric approach to understanding the generation of wadi flash floods. *Water* **2017**, *9*, 553. [CrossRef]
3. Milewski, A.; Sultan, M.; Yan, E.; Becker, R.; Abdeldayem, A.; Soliman, F.; Abdel Gelil, K. A remote sensing solution for estimating runoff and recharge in arid environments. *J. Hydrol.* **2009**, *373*, 1–14. [CrossRef]
4. Moneim, A.A. Hydrogeological conditions and aquifers potentiality for sustainable development of the desert areas in Wadi Qena, Eastern Desert. *Egypt. Arab. J. Geosci.* **2014**, *7*, 4573–4591. [CrossRef]
5. Aggour, T.A. Impact of Geomorphological and Geological Setting on Groundwater in Qena-Safaga District, Central Eastern Desert, Egypt. Ph.D. Thesis, Faculty of Science, Ain Shams University, Cairo, Egypt, 1997; p. 355.
6. Moneim, A.A. Overview of the geomorphological and hydrogeological characteristics of the Eastern Desert of Egypt. *Hydrogeol. J.* **2005**, *13*, 416–425. [CrossRef]
7. Negrel, P.; Lemiere, B.; de Grammont, H.M.; Billaud, P.; Sengupta, B. Hydrogeochemical processes, mixing and isotope tracing in hard rock aquifers and surface waters from the Subarnarekha River basin, (east Singhbhum District, Jharkhand state, India). *Hydrogeol. J.* **2007**, *15*, 1535–1552. [CrossRef]

8. Londono, O.M.Q.; Martinez, D.E.; Dapena, C.; Massone, H. Hydrogeochemistry and isotope analyses used to determine groundwater recharge and flow in low-gradient catchments of the province of Buenos Aires, Argentina. *Hydrogeol. J.* **2008**, *16*, 1113–1127. [CrossRef]
9. Wang, L.; Dong, Y.; Xu, Z.; Qiao, X. Hydrochemical and isotopic characteristics of groundwater in the north-eastern Tennger Desert, northern China. *Hydrogeol. J.* **2017**, *25*, 2363–2375. [CrossRef]
10. Sami, K. Recharge mechanisms and geochemical processes in a semi-arid sedimentary basin, Eastern Cape, South Africa. *J. Hydrol.* **1992**, *139*, 27–48. [CrossRef]
11. Schuh, W.M.; Klinkebiel, D.L.; Gardner, J.C.; Meyer, R.F. Tracer and Nitrate Movement to Groundwater in the Northern Great Plains. *J. Environ. Qual.* **1997**, *26*, 1335–1347. [CrossRef]
12. Aghazadeh, N.; Mogaddam, A.A. Investigation of hydrochemical characteristics of groundwater in the Harzandat aquifer, Northwest of Iran. *Environ. Monit. Assess.* **2011**, *176*, 183–195. [CrossRef]
13. Kuldip, S.; Hundal, H.S.; Dhanwinder, S. Geochemistry and assessment of hydrogeochemical processes in groundwater in the Southern part of Bathinda district of Punjab, northwest India. *Environ. Earth Sci.* **2011**, *64*, 1823–1833. [CrossRef]
14. Cloutier, V.; Lefebvre, R.; Savard, M.M.; Bourque, E.; Therrien, R. Hydrogeochemistry and groundwater origin of the Basses–Laurentides sedimentary rock aquifer system, St. Lawrence Lowlands, Quebec, Canada. *Hydrogeol. J.* **2006**, *14*, 573–590. [CrossRef]
15. Eissa, M.A.; Thomas, J.M.; Pohll, G.; Hershey, R.L.; Dahab, K.A.; Dawoud, M.I.; ElShiekh, A.; Gomaa, M.A. Groundwater resource sustainability in the Wadi Watir Delta, Gulf of Aqaba, Sinai, Egypt. *Hydrogeol. J.* **2013**, *21*, 1833–1851. [CrossRef]
16. Eissa, M.A.; Shawky, H.; Samy, A.; Khalil, M.M.; El Malky, M. Geochemical and Isotopic Evidence of Groundwater Salinization Processes in El Dabaa Area, Northwestern Coast, Egypt. *Geosciences* **2018**, *8*, 392. [CrossRef]
17. Eissa, M.; Ali, M.; Zaghlool, E.; Stash, O.S. Hydrochemical and stable isotopes indicators for detecting sources of groundwater contamination close to Bahr El-Baqar drain, eastern Nile Delta, Egypt. *Water Sci.* **2019**, *33*, 54–64. [CrossRef]
18. Mook, W. Environmental isotopes in the hydrological cycle: Principles and applications. In *Introduction: Theory, Methods*; International Atomic Energy Agency (IAEA): Vienna, Austria, 2000.
19. Subyani, A.M. Use of chloride-mass balance and environmental isotopes for evaluation of groundwater recharge in the alluvial aquifer, Wadi Tharad, western Saudi Arabia. *Environ. Geol.* **2004**, *46*, 741–749. [CrossRef]
20. Lapworth, D.J.; MacDonald, A.M.; Tijani, M.N.; Darling, W.G.; Gooddy, D.C.; Bonsor, H.C.; Araguas-Araguas, L.J. Residence times of shallow groundwater in West Africa: Implications for hydrogeology and resilience to future changes in climate. *Hydrogeol. J.* **2013**, *21*, 673–686. [CrossRef]
21. Wang, L. Sea lanes and Chinese national energy security. *J. Coast. Res.* **2015**, *73*, 572–576. [CrossRef]
22. Wang, L.; Quant, R.; Kolios, A. Fluid structure interaction modelling of horizontal-axis wind turbine blades based on CFD and FEA. *J. Wind. Eng. Ind. Aerodyn.* **2016**, *158*, 11–25. [CrossRef]
23. Moneim, A.A.; Seleem, E.M.; Zeid, S.A.; Samie, S.A.; Zaki, S.; El-Fotoh, A.A. Hydrogeochemical characteristics and age dating of groundwater in the Quaternary and Nubian aquifer systems in Wadi Qena, Eastern Desert, Egypt. Sustain. *Water Resour. Manag.* **2015**, *1*, 213–232.
24. Hussien, M.H.; Kehew, A.E.; Aggour, T.A.; Korany, E.; Abotalib, Z.A.; Hassanein, A.; Morsy, S. An integrated approach for identification of potential aquifer zones in structurally controlled terrain: Wadi Qena basin, Egypt. *Catena* **2017**, *149*, 73–85. [CrossRef]
25. Hussien, M.H. Development of The Water Resources In Wadi Qena Basin, Eastern Desert, Egypt. Ph.D. Thesis, Faculty of Science Ain Shams University, Cairo, Egypt, 2017.
26. Issawi, B.; Jux, U. Contributions to the stratigraphy of the paleozoic rocks in Egypt. *Egypt. Geol. Surv.* **1982**, *62*, 28.
27. Soliman, M.A.; Habib, M.F.; Ahmed, E.A. Sedimentologic and tectonic evolution of the Upper Cretaceous-Lower Tertiary succession at Wadi Qena, Egypt. *Sediment. Geol.* **1986**, *46*, 111–133. [CrossRef]
28. Said, R. *The Geology of Egypt*; Balkema/Rotterdam/Brookfield: Amsterdam, The Netherlands, 1990; p. 734.
29. El Basely, M.I. Quaternary Geology of Some Selected Drainage Basins in Upper Egypt (Qena-Idfu Area). Ph.D. Thesis, Cairo University, Cairo, Egypt, 1994; p. 242.
30. Hendriks, F.; Kallenbach, H.; Philobbos, E.R. Cretaceous to Early Tertiary Continental and marginal marine sedimentary environments of southeastern Egypt. *J. Afr. Earth Sci.* **1990**, *10*, 229–241. [CrossRef]
31. Nagm, E.; Wilmsen, M. Studied Late Cenomanian–Turonian (Cretaceous) ammonites from Wadi Qena, central Eastern Desert, Egypt: Taxonomy, bio- stratigraphy and palaeobiogeographic implications. *Acta Geol. Pol.* **2012**, *62*, 63–89.
32. El-Gaby, S.; List, F.K.; Tehrani, R. Geology, evolution and metallogenesis of the Pan-African belt in Egypt. In *The Pan-African Belt of Northeast Africa and Adjacent Areas: Tectonic Evolution and Economic Aspects of a Late Proterozoic Oregon*; F. Vieweg: Berlin, Germany, 1988; pp. 17–68.
33. Sultan, M.; Arvidson, R.E.; Duncan, I.J.; Stern, R.J.; El Kaliouby, B. Extension of the Najd shear system from Saudi Arabia to the Central Eastern Desert of Egypt based on integrated field and Landsat observations. *Tectonics* **1988**, *7*, 1291–1306. [CrossRef]
34. Akawy, A. Structural geomorphology and neotectonics of the Qina-Safaja district, Egypt. *Neues Jahrb. Geol. Paläontologie-Abh.* **2002**, *226*, 95–130. [CrossRef]
35. Akawy, A.; El-Din, K.G. Middle Eocene to recent tectonics in the Qina area, Upper Egypt. *Neues Jahrb. Geol. Paläontologie-Abh.* **2006**, *240*, 19–51. [CrossRef]

36. CONOCO. *Geological Map of Egypt, Scale 1: 500,000, Assiut and Beni Suef*; The Egyptian General Petroleum Corporation (EGPC): Cairo, Egypt, 1987.
37. General Authority for Rehabilitation Projects and Agricultural Development (GARPAD). Wadi El Matulli, Hydrogeological studies. *Catena* **2017**, *149*, 73–85. (In Arabic)
38. Research Institute of Groundwater (RIGW). *Hydrogeological map of Wadi Qena*; RIGW: Cairo, Egypt, 1998.
39. ASTM (American Society for Testing and Materials). *Annual Book of ASTM Standards*; ASTM: Baltimore, MD, USA, 2002; Volume 11, 939p.
40. Richards, I.A. *Diagnosis and Improvement of Saline and Alkali Soils, Handbook No. 60*; United States Department of Agriculture (USDA): Washington, DC, USA, 1954; p. 160.
41. Plummer, L.N.; Prestemon, E.C.; Parkhurst, D.L. An interactive code (NETPATH) for modeling net geochemical reactions along a flow path, version 2.0. *Water-Resour. Investig. Rep.* **1994**, *94*, 4169.
42. Yousif, M.; Oguchi, T.; Anazawa, K.; Ohba, T. Geospatial Information and Environmental Isotopes for Hydrogeological Evaluation: Ras Alam El Rum, Northwestern Coast of Egypt. *Nat. Resour. Res.* **2014**, *23*, 423–445. [CrossRef]
43. Bloomfield, J.P.; Jackson, C.R.; Stuart, M.E. Changes in groundwater levels, temperature and quality in the UK over the 20th century: An assessment of evidence of impacts from climate change. In *A Climate Change Report Card for Water Working Technical Paper*; British Geological Survey, Kingsley Dunham Centre: Keyworth, UK, 2013; p. 14.
44. Drever, J. *The Geochemistry of Natural Water, Surface and Ground Water Environments*, 3rd ed.; Prentice Hall: Hoboken, NJ, USA, 1997; p. 436.
45. Chebotarev, I.I. Metamorphism of natural waters in the crust of weathering. *Geochim. Cosmochim. Acta* **1955**, *8*, 137–170 & 198–212. [CrossRef]
46. Piper, A.M. A graphic procedure in the geochemical interpretation of water analysis. *Eos Trans. Am. Geophys.* **1944**, *25*, 914–928. [CrossRef]
47. Hem, J.D. *Study and Interpretation of the Chemical Characteristics of Natural Water*; Department of the Interior, US Geological Survey: St. Alexandria, VA, USA, 1985; p. 2254.
48. Mohallel, S.A. Applications of Hydrogeochemical Modeling to Evaluate Water Resources in the Area between Edfu and Aswan, Eastern Desert, Egypt. Ph.D. Thesis, Faculty of Science (Boys) Al-Azhar University, Cairo, Egypt, 2013.
49. Dansgaard, W. *Stable Isotopes in Precipitation*; Wiley: Hoboken, NJ, USA, 1964; Volume 16, pp. 436–468.
50. Clark, I.; Fritz, P. Nitrogen cycling in rural watershed. In *Environmental Isotopes in Hydrogeology*; CRC Press: Boca Raton, FL, USA, 1997; pp. 148–151.
51. Mohammed, A.M.; Krishnamurthy, R.V.; Kehew, A.E.; Crossey, L.J.; Karlstrom, K.K. Factors affecting the stable isotopes ratios in groundwater impacted by intense agricultural practices: A case study from the Nile Valley of Egypt. *Sci. Total Environ.* **2016**, *15*, 707–715. [CrossRef] [PubMed]
52. Craig, H. Isotopic variations in meteoric waters. *Science* **1961**, *133*, 1702–1703. [CrossRef] [PubMed]
53. Gibbs, R.J. Mechanisms controlling world's water chemistry. *Science* **1970**, *170*, 1088–1090. [CrossRef] [PubMed]
54. Sukhija, B.S.; Varma, V.N.; Nagabhushanam, P.; Reddy, D.V. Differentiation of palaeomarine and modern seawater intruded salinities in coastal groundwaters (of Karaikal and Tanjavur, India) based on inorganic chemistry, organic biomarker fingerprints and radiocarbon dating. *J. Hydrol.* **1996**, *174*, 173–201. [CrossRef]
55. Vengosh, A.; Spivack, A.J.; Artzi, Y.; Ayalon, A. Geochemical and boron, strontium, and oxygen isotopic constraints on the origin of the salinity in groundwater from the Mediterranean coast of Israel. *Water Resour. Res.* **1999**, *35*, 1877–1894. [CrossRef]
56. El Moujabber, M.; Samra, B.B.; Darwish, T.; Atallah, T. Comparison of different indicators for groundwater contamination by seawater intrusion on the Lebanese coast. *Water Resour. Manag.* **2006**, *20*, 161–180. [CrossRef]
57. Kouzana, L.; Mammou, A.B.; Felfoul, M.S. Seawater intrusion and associated processes: Case of the Korba aquifer (Cap-Bon, Tunisia). *Comptes Rendus Geosci.* **2009**, *341*, 21–35. [CrossRef]
58. Mayback, M. Global chemical weathering of surficial rocks estimated from river dissolved loads. *Am. J. Sci.* **1987**, *287*, 401–428. [CrossRef]
59. Hershey, R.L.; Heilweil, V.M.; Gardner, P.; Lyles, B.F.; Earman, S.; Thomas, J.M.; Lundmark, K.W. *Ground-Water Chemistry Interpretations Supporting the Basin and Range Regional Carbonate-Rock Aquifer System (BARCAS) Study, Eastern Nevada and Western Utah*; Desert Research Institute: Reno, NV, USA, 2007; p. 86.
60. Back, W.; Hanshaw, B.B.; Plummer, L.N.; Rahn, P.H.; Rightmire, C.T.; Rubin, M. Process and rate of dedolomitization: Mass transfer and 14C dating in a regional carbonate aquifer. *Geol. Soc. Am. Bull.* **1983**, *94*, 1415–1429. [CrossRef]